

# Spatiotemporal 2-D Channel Coding for Very Low Latency Reliable MIMO Transmission

Xiaohu You, *Fellow, IEEE*, Chuan Zhang, *Senior Member, IEEE*, Bin Sheng, Yongming Huang, *Senior Member, IEEE*, Chen Ji, Yifei Shen, Wenyue Zhou, and Jian Liu

**Abstract**—To fully support vertical industries, 5G and its corresponding channel coding are expected to meet requirements of different applications. However, for applications of 5G and beyond 5G (B5G) such as URLLC, the transmission latency is required to be much shorter than that in eMBB. Therefore, the resulting channel code length reduces drastically. In this case, the traditional 1-D channel coding suffers a lot from the performance degradation and fails to deliver strong reliability with very low latency. To remove this bottleneck, new channel coding scheme beyond the existing 1-D one is in urgent need. By making full use of the spacial freedom of massive MIMO systems, this paper devotes itself in proposing a spatiotemporal 2-D channel coding for very low latency reliable transmission. For a very short time-domain code length  $N^{\text{time}} = 16, 64 \times 128$  MIMO system employing the proposed spatiotemporal 2-D polar channel coding scheme successfully shows more than 3 dB performance gain at FER =  $10^{-3}$ , compared to the 1-D time-domain channel coding. It is noted that the proposed coding scheme is suitable for different channel codes and enjoys high flexibility to adapt to difference scenarios. By appropriately selecting the code rate, code length, and the number of codewords in the time and space domains, the proposed coding scheme can achieve a good trade-off between the transmission latency and reliability.

**Index Terms**—Channel coding, spatiotemporal, low latency, high reliability, MIMO.

## I. INTRODUCTION

WITH its rapid development, wireless communications now ranks as a key driver of economic and social progress. Officially commercialized in the year of 2019 [1], the fifth generation network (5G) of cellular mobile communications has become the leading part of the “new infrastructure”, and greatly transforms vertical industries. To fulfill the demands of different vertical applications, 5G is sliced into three use cases: enhanced mobile broadband (eMBB), ultra-reliable low-latency communications (URLLC), and massive machine type communications (mMTC) [2, 3]. As one of the most crucial parts of baseband processing, channel coding for 5G now faces challenging requirements on flexibility, decoding performance, decoding latency, implementation complexity, and so on. One well-known example is the eMBB case adopts two kind of channel codes at the same time: low-density parity-check (LDPC) codes used for data channels, and polar codes used for control channels [4, 5].

X. You, C. Zhang, B. Sheng, Y. Huang, Y. Shen, W. Zhou, and J. Liu are with the National Mobile Communications Research Laboratory, Southeast University, Nanjing 211189, China, and also with the Purple Mountain Laboratories, Nanjing 211189, China. email: {xhyu, chzhang}@seu.edu.cn. (*Corresponding authors: Xiaohu You and Chuan Zhang.*)

C. Ji is with the School of Information Science and Technology, Nantong University, Nantong 226019, China.

However, in order to achieve the goals set for 5G, such hybrid channel coding setup is far from enough. Further enabling channel coding schemes are expected. One existing challenge is the implementation of very low latency reliable multiple-input multiple-output (MIMO) transmission for URLLC. In the eMBB case, both channel codes (LDPC codes and polar codes) are coded in one dimension, time domain. Admittedly, this 1-D coding is acceptable for eMBB, since the corresponding package length is sufficiently long for both LDPC codes and polar codes to deliver satisfactory decoding performance [3]. Unfortunately, for URLLC, in order to lower the latency, the package length is much reduced [3, 6]. Consequently, the decoding performance heavily degrades and the transmission reliability is no longer guaranteed. Therefore, new coding schemes which can flexibly balance both transmission reliability and decoding latency is highly required.

On the other hand, it is noticed that massive MIMO technology is another enabling technique for 5G besides channel coding [7]. It brings considerable advantages in both spectral efficiency (SE) and energy efficiency (EE). For channel codes, the massiveness of antennas offers another dimension, space domain for encoding [8]. This enables us to propose a spatiotemporal 2-D channel coding to implement very low latency reliable data transmission for 5G. The proposed scheme introduce the space-domain coding over the current time-domain coding. With very short time-domain code length, it can greatly improve the decoding performance. This scheme cannot only meet URLLC’s requirements on latency, reliability, and transmission rate, but also enjoy perfect flexibility for applications in various scenarios.

The contributions of this paper are as follows.

- Making use of both the time domain and space domain of massive MIMO systems, this paper proposes a spatiotemporal 2-D channel coding scheme which can well balance transmission latency and reliability.
- A configuration method by leveraging the layer mapping, code length, code rate to flexibly meet requirements of different applications scenarios including eMBB and URLLC is proposed.
- The proposed scheme is general, regular, and implementation-friendly. It can be applied to any existing MIMO systems without touching the other modules and has wide application prospect.

The remainder of this paper is organized as follows. Section II introduces the multi-antenna baseband transmitting systems, where the layer mapping and time-domain 1-D coding

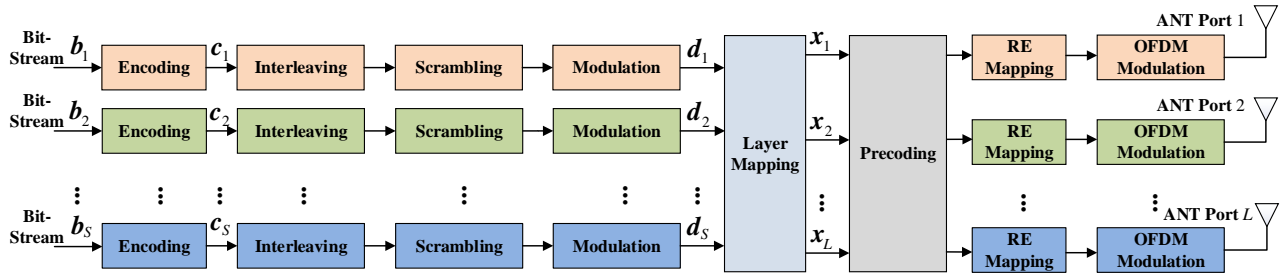


Fig. 1. The block diagram of the multi-antenna baseband transmitting system.

are described in detail. Section III proposes the spatiotemporal 2-D channel coding scheme with the corresponding baseband system and latency analysis. Numerical results are provided in Section IV. The advantages of the proposed coding scheme are discussed in Section V and Section VI concludes this paper.

## II. PRELIMINARIES

In this section, a brief introduction of the traditional multi-antenna baseband transmitting system, the layer mapping, and the time-domain 1-D channel coding scheme is given. Since this paper is on the channel coding scheme, we mainly focus on the corresponding transmitting system. Readers who would like to see more details of the entire system including the receiving part, can refer to Fig. 1 of [9].

### A. Multi-Antenna Baseband Transmitting Systems

In the physical (PHY) layer of wireless systems, the transmission block (TB) from the media access control (MAC) layer is transferred into multiple orthogonal frequency division multiplexing (OFDM) symbols and then transmitted via multiple antenna ports (ANT ports). The details of a multi-antenna baseband transmitting system are illustrated in Fig. 1.

The input TB is first divided into several bit-streams  $\{\mathbf{b}_s\}$ , where  $1 \leq s \leq S$  and  $S$  is the cardinality of  $\{\mathbf{b}_s\}$ . Each bit-stream  $\mathbf{b}_s$  is of length  $K_s$ , and will be encoded into a codeword  $\mathbf{c}_s$  of length  $N_s$  and rate  $R_s = K_s/N_s$ . After the operations of interleaving, scrambling, and modulation,  $\mathbf{c}_s$  is mapped to a complex-valued symbol sequence  $\mathbf{d}_s$ . For different modulation schemes, each symbol corresponds to different number of bits. For instance, with  $2^q$ -quadrature amplitude modulation (QAM), each symbol of  $\mathbf{d}_s$  is mapped from  $q$  continuous bits.

For air interface transmission, those symbols are mapped to ANT ports by layer mapping, precoding, resource element (RE) mapping, and OFDM modulation. The detailed steps are as follows.

By layer mapping,  $\mathbf{d}_s$  is allocated into several layers out of totally  $L$  layers. Without loss of generality, in this paper it is assumed that the number of layers is same as the number of ANT ports and the number of transmitting antennas (Fig. 1). In Layer  $l$  ( $1 \leq l \leq L$ ), the symbol sequence is denoted as  $\mathbf{x}_l$ , which is further precoded with the precoding matrix. The precoded symbols are first scaled with the amplitude factor regarding the transmitting power, and then mapped to the REs. Finally, these scaled symbols are modulated to orthogonal

subcarriers, and transmitted via ANT ports in the synthetic OFDM symbols [10]. In the aforementioned steps, the layer mapping is of good relevance of the proposed channel coding scheme and is detailed in the following sub-section.

### B. Layer Mapping

The layer mapping scheme is proposed due to the inherently differentiated demands of wireless communications. In practice, the wireless systems will involve different users/tasks, and different users/tasks need to meet different requirements. Therefore, layer mapping enables us to apply different schemes such as channel coding schemes (i.e., code type, code rate, code length, and so on) in different layers. In real applications, there are two mainstream layer mapping schemes, namely 1) the folded layer mapping and 2) the parallel layer mapping.

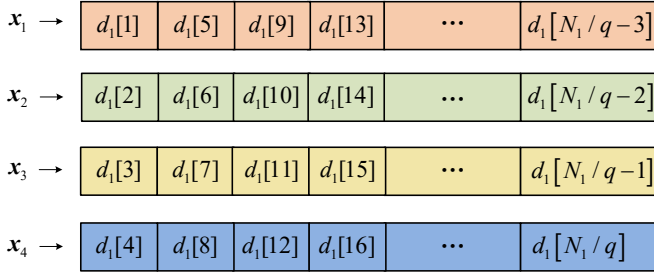
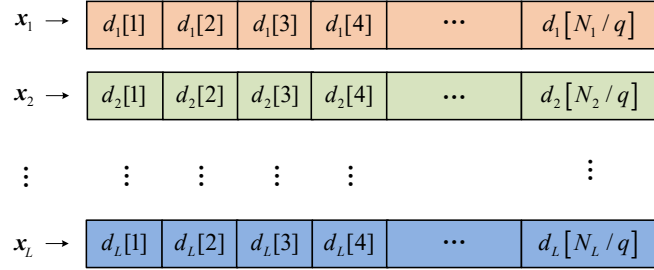
1) *Folded Layer Mapping*: Since the implementation cost increases linearly with the number of bit-streams ( $S$ ), in traditional applications which are sensitive to complexity, there is sometimes a constraint on  $S$ . For example, the current 5G NR sets the maximum number of bit-streams as 2 [11]. Therefore, it holds that  $S < L$  and the layer mapping needs to be done by folding one bit-stream into multiple layers. Fig. 2 shows an example of the folded layer mapping with  $L = 4$  and  $S = 1$ , which is compatible with the current 5G NR.

2) *Parallel Layer Mapping*: However, with the progressive evolution of 5G NR, implementation complexity is no longer the key bottleneck. And the existing folded layer mapping shows disadvantages such as high latency and low flexibility. Though straightforward but efficient, the parallel layer mapping becomes favorable. In this scheme, the number of layers ( $L$ ) is set the same as the number of bit-streams ( $S$ ). More specifically, for the parallel layer mapping, we have  $S = L$  and  $\mathbf{x}_l = \mathbf{d}_s$  for  $\forall l = s$ . Therefore, all bit-streams can be encoded independently and in parallel, which reduces latency and improves both flexibility and coding efficiency. Illustration of the parallel layer mapping is given by Fig. 3.

### C. Time-Domain 1-D Channel Coding

According to Section II-A, it can be seen that for either the parallel layer mapping or the folded layer mapping, the channel coding is done in 1-D time domain. Taking the parallel layer mapping as an example, the time-domain codewords are of length  $N_s$  and rate  $R_s = K_s/N_s$ .

Admittedly, the current time-domain 1-D channel coding scheme can sufficiently meet the requirements posed by eMBB.

Fig. 2. The illustration of the folded layer mapping with  $L = 4$  and  $S = 1$ .Fig. 3. The illustration of the parallel layer mapping, where  $S = L$ .

However, for other applications such as URLLC, which requires very low latency and ultra-reliable transmission, the time-domain channel coding scheme no longer serves. For URLLC, in order to meet the latency requirement, the package length or codeword length ( $N_s$ ) should be much shorter than that in eMBB, which will inevitably reduce the transmission reliability. According to Fig. 4, even for the parallel layer mapping, the frame error rate (FER) performance of 1-D time-domain coding degrades severely as  $N_s$  reduces. In this plot, polar code using Tal-Vardy construction [12] is chosen as the channel code and the MIMO antenna configuration is  $N_t \times N_r = 64 \times 128$ . The modulation scheme is 16-QAM. The polar decoder is the successive cancellation (SC) decoder [13]. The MIMO detector is the minimum mean square error (MMSE) detector [14]–[16]. Without loss of generality, the above configuration is adopted as the running setup for the following simulations, unless specified additionally.

Therefore, new channel coding schemes which can offer very low latency and ultra-reliable transmission are in urgent need. To this end, the rest of this paper proposes a spatiotemporal 2-D channel coding scheme.

### III. PROPOSED SPATIOTEMPORAL 2-D CHANNEL CODING

In this section, the proposed spatiotemporal 2-D channel coding scheme is introduced with details. Its flexibility and latency analysis are also given.

#### A. Multi-Antenna Transmitting Systems with 2-D Coding

To address the contradiction between latency and reliability of 1-D coding, we need to revisit the multi-antenna transmitting systems in Fig. 1. For massive MIMO systems, the number of ANT ports ( $L$ ) is relatively large and provides us another

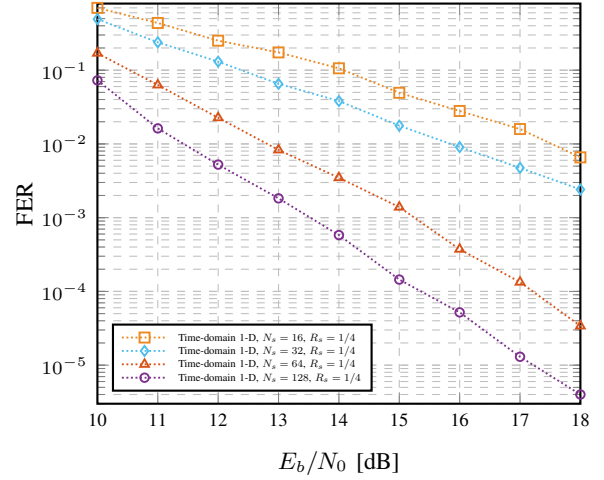


Fig. 4. FER performance of time-domain 1-D channel coding with decreasing code lengths.

dimension for operation, i.e. the space domain. This inspires us to improve the reliability by making use of the already existing antenna massiveness. The proposed scheme is named spatiotemporal 2-D channel coding scheme, which introduces the space-domain coding over the current time-domain coding. This scheme cannot only meet URLLC's requirements on latency, reliability, and transmission rate, but also enjoy perfect flexibility for applications in various scenarios.

Fig. 5 shows the details of a multi-antenna baseband transmitting system with 2-D channel coding. Compared to the system in Fig. 1, the Encoding modules have been replaced by a Spatiotemporal 2-D Coding module, whereas the other modules stay unchanged. In general, the proposed spatiotemporal 2-D coding can be directly applied to any 1-D coded systems without touching the other modules except the coding module. Therefore, this scheme expects wide applications. Similar to the 1-D coded system in Fig. 1, the Layer Mapping module distributes the complex-valued symbols in  $L$  layers. In each layer, the number of symbols is  $M_{\text{sym}}$ . In practice,  $M_{\text{sym}}$  is determined by the input length of the system and bounded by the number of subcarriers, which is very small for URLLC.

Before giving details of the spatiotemporal 2-D channel coding scheme, the concept of the codeword trellis is introduced in the next subsection.

#### B. Codeword Trellis

In each layer,  $M_{\text{sym}}$  complex-valued symbols are mapped from  $M_{\text{bit}} = qM_{\text{sym}}$  coded bits. Therefore, the codewords before modulation form a (bit-level) *codeword trellis*, whose width and height are  $M_{\text{bit}}$  and  $L$ , respectively.

Assume the area of the TB is fixed. Given the transmission latency ( $M_{\text{bit}}$ ) and the number of layers ( $L$ ), different coding schemes result in different distributions of information bits in the codeword trellis. And therefore, different decoding performances (transmission reliability) are obtained. The key task of us is to find out the distribution, which can well balance transmission latency and reliability. The codeword trellis is a

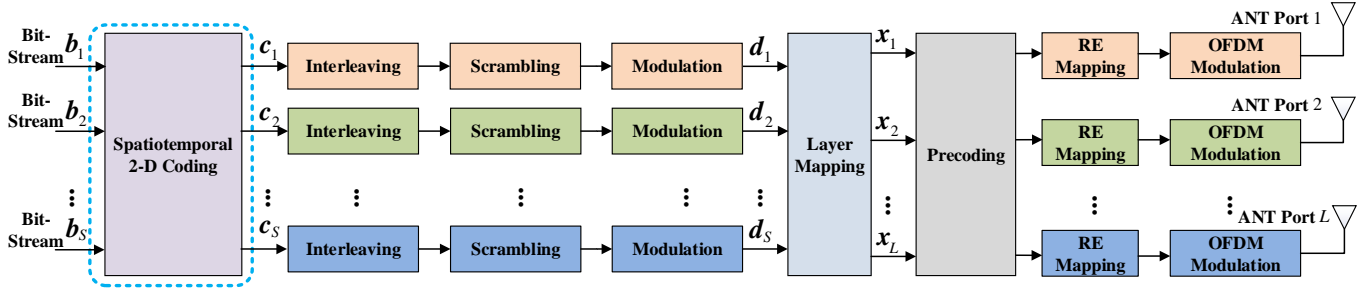


Fig. 5. The block diagram of the multi-antenna baseband transmitting system with the spatiotemporal 2-D coding.

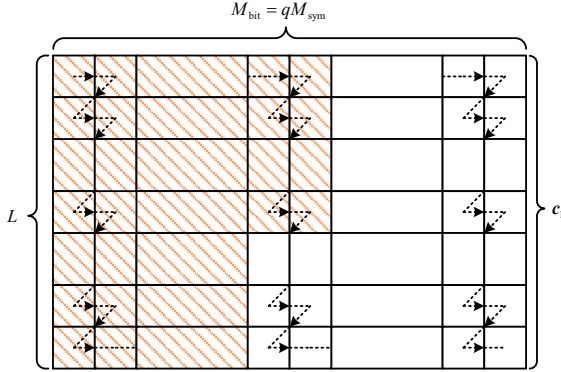


Fig. 6. The codeword trellis of the folded layer mapping with  $S = 1$ .

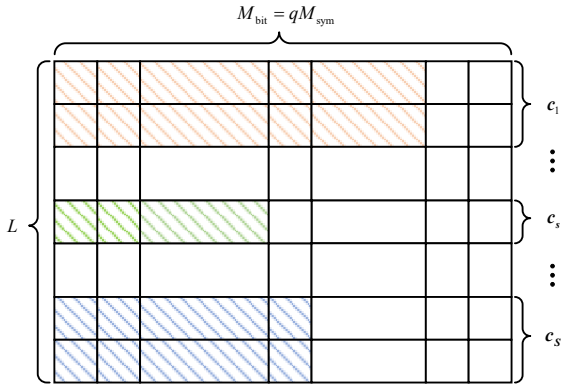


Fig. 7. The codeword trellis of the parallel layer mapping with flexibility, when  $S = L$  it corresponds to Fig. 3.

generalized representation of the illustrations in both Figs 2 and 3. For example, the codeword trellis of the folded layer mapping is in Fig. 6, where 4-QAM is employed and information bits are shaded. And the codeword trellis of the parallel layer mapping is shown in Fig. 7. The rest part of this paper employs the codeword trellis extensively.

### C. Spatiotemporal 2-D Channel Coding

As discussed previously, for URLLC the transmission latency reduces and  $S$  increases. The resulting degraded reliability is now compensated by the space-domain coding. Herein, we introduce the spatiotemporal 2-D channel coding scheme with the help of codeword trellis. We first consider the time-space

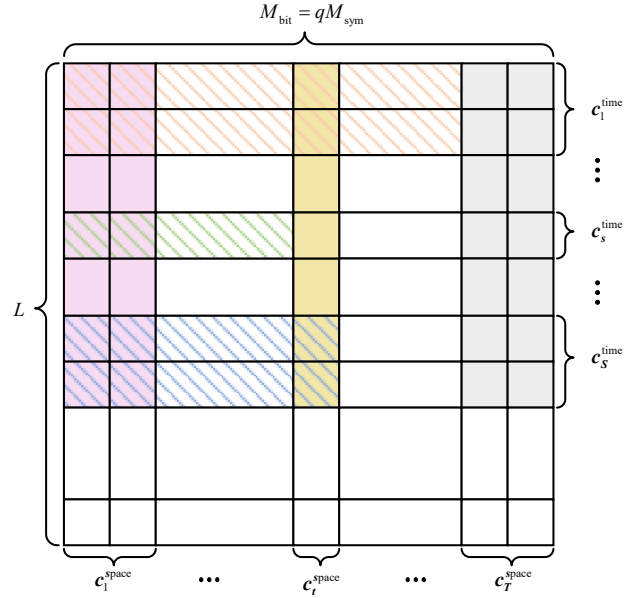


Fig. 8. The codeword trellis of the spatiotemporal 2-D channel coding.

mode: the time-domain coding is performed first, followed by the space-domain coding. The number of codewords in time domain is  $S$  and the number of codewords in space domain is  $T$ .

The codeword trellis of the time-space mode is shown in Fig. 8. In the time domain, the  $S$  bit-streams  $\{b_s\}$  are first encoded to  $S$  codewords  $\{c_s^{\text{time}}\}$ , where  $1 \leq s \leq S$ . For each codeword  $c_s^{\text{time}}$ , the length and rate are  $N_s^{\text{time}}$  and  $R_s^{\text{time}}$ , respectively. It is noted that the rate-matching is required to make sure  $N_s^{\text{time}}$  is a multiple of  $M_{\text{bit}}$ , so that the codeword  $c_s^{\text{time}}$  is mapped to  $N_s^{\text{time}}/M_{\text{bit}}$  layers. Similarly, in the space domain, there are  $T$  codewords  $\{c_t^{\text{space}}\}$ , whose lengths  $N_t^{\text{space}}$  and rates  $R_t^{\text{space}}$  can be different ( $1 \leq t \leq T$ ). The rate-matching is also required in the space domain.

The code type, code rate, and code length of each codeword in either time or space domain can be flexibly determined upon the requirements. At the receiving system, the log-likelihood ratios (LLRs) of each  $c_t^{\text{space}}$  are obtained first, by  $T$  soft-output decoders. After the space-domain decoding, the LLRs of each  $c_s^{\text{time}}$  are obtained and  $S$  decoders are activated to recover the information bits.

**Example:** For better understanding of the proposed scheme,

an example with  $M_{\text{bit}} = 16$  and  $L = 64$  is given here. Suppose there are 256 information bits  $\{a_1 \dots a_{256}\}$  in the TB, which are lined in parallel to form 32 bit-streams. Assume three code rates are required according to the feedback from the receiver, which are 1/4 for  $\{\mathbf{b}_1 \dots \mathbf{b}_{10}\}$ , 1/2 for  $\{\mathbf{b}_{11} \dots \mathbf{b}_{22}\}$ , and 3/4 for  $\{\mathbf{b}_{23} \dots \mathbf{b}_{32}\}$ . The bit-streams are explicitly given as follows:

$$\left\{ \begin{array}{l} \mathbf{b}_1 = [a_1, a_2, a_3, a_4], \\ \vdots \\ \mathbf{b}_{10} = [a_{37}, a_{38}, a_{39}, a_{40}], \\ \mathbf{b}_{11} = [a_{41}, a_{42}, a_{43}, a_{44}, a_{45}, a_{46}, a_{47}, a_{48}], \\ \vdots \\ \mathbf{b}_{22} = [a_{129}, a_{130}, a_{131}, a_{132}, a_{133}, a_{134}, a_{135}, a_{136}], \\ \mathbf{b}_{23} = [a_{137}, a_{138}, \dots, a_{148}], \\ \vdots \\ \mathbf{b}_{32} = [a_{244}, a_{245}, \dots, a_{256}]. \end{array} \right. \quad (1)$$

Based on the specified coding scheme, 32 codewords are generated with the same code length  $N^{\text{time}} = 16$ .

$$\mathbf{c}^{\text{time}} = \begin{bmatrix} \mathbf{c}_1^{\text{time}} \\ \mathbf{c}_2^{\text{time}} \\ \vdots \\ \mathbf{c}_{32}^{\text{time}} \end{bmatrix} = \begin{bmatrix} \mathbf{c}_1^{\text{time}}[1] & \mathbf{c}_1^{\text{time}}[2] & \dots & \mathbf{c}_1^{\text{time}}[16] \\ \mathbf{c}_2^{\text{time}}[1] & \mathbf{c}_2^{\text{time}}[2] & \dots & \mathbf{c}_2^{\text{time}}[16] \\ \vdots & \vdots & \ddots & \vdots \\ \mathbf{c}_{32}^{\text{time}}[1] & \mathbf{c}_{32}^{\text{time}}[2] & \dots & \mathbf{c}_{32}^{\text{time}}[16] \end{bmatrix}. \quad (2)$$

Further, each column is encoded in the space domain with the same code rate  $R^{\text{space}} = 1/2$ ,

$$\mathbf{c}_t^{\text{space}} = [\mathbf{c}_1^{\text{time}}[t], \dots, \mathbf{c}_{32}^{\text{time}}[t]] \cdot \mathbf{G}^{\text{space}}, \quad 1 \leq t \leq 16, \quad (3)$$

where  $\mathbf{G}^{\text{space}}$  is the generator matrix of the codeword in the space domain.

It is noted that we can also perform the space-domain coding first, then the time-domain coding. This mode is named space-time mode. Consequently, the receiver first takes care of the time-domain decoding, then the space-domain decoding.

#### D. Latency Analysis

According to the above analysis, different coding schemes over the same codeword trellis have the same transmission latency but different decoding latencies. In pipelined transmission, the transmission process and decoding process are overlapped. Therefore, the resulting latency is calculated in a synthetic manner with the following three assumptions:

1) The decoding cannot start unless the LLRs of a complete codeword trellis are received.

2) All decoders in the same domain can work in parallel.

3) The latency of decoding a codeword  $\mathbf{c}_s$  is proportional to the code length, as  $\mathcal{D}(\mathbf{c}_s) = \gamma \cdot N_s$  (SC polar decoder is assumed).

Therefore, the decoding latency of the proposed spatiotemporal 2-D channel coding scheme is:

$$\mathcal{D} = \gamma \cdot \left( \max_{1 \leq s \leq S} \{N_s^{\text{time}}\} + \max_{1 \leq t \leq T} \{N_t^{\text{space}}\} \right). \quad (4)$$

The lowest latency  $\mathcal{D}_{\text{min}} = \gamma \cdot (M_{\text{bit}} + L)$  is achieved when each codeword in the time/space domain takes up exactly one row/column of the codeword trellis. The decoding latency increases as  $S$  or  $T$  decreases.

The coding schemes in Figs. 6 and 7 are two special cases of the proposed spatiotemporal 2-D channel coding scheme. In Fig. 6, we have  $S = L$  and  $R_t^{\text{space}} = 1$ . Its decoding latency is  $\mathcal{D} = \gamma \cdot (M_{\text{bit}})$ , which is low but with a poor decoding performance as shown in Fig. 4. In Fig. 7, no space-domain coding is involved and  $S = 1$ . Its decoding latency is  $\mathcal{D} = \gamma \cdot (L \cdot M_{\text{bit}})$ , which is very long. Therefore, spatiotemporal 2-D channel coding scheme considering both time and space domain coding is a good choice for balancing latency and reliability.

## IV. NUMERICAL RESULTS

In this section, numerical results are provided to demonstrate the advantages of the proposed spatiotemporal 2-D channel coding scheme. The simulation setup keeps the same as that of Fig. 4 unless specified additionally. In order to achieve the lowest latency  $\mathcal{D}_{\text{min}} = \gamma \cdot (M_{\text{bit}} + L)$ , it is assumed that each codeword in the time/space domain takes up exactly one row/column of the codeword trellis. The corresponding time/space-domain code length and code rate are  $N^{\text{time}}/N^{\text{space}}$  and  $R^{\text{time}}/R^{\text{space}}$ , respectively.

#### A. Spatiotemporal 2-D Coding Improves the Reliability

According to the results shown in Fig. 9, it is clear that the introduction of spatiotemporal 2-D coding will consistently bring reliability advantages for different time-domain code lengths. For comparison fairness, the spatiotemporal 2-D coding keeps the same time-domain code length ( $N^{\text{time}}$ ) and overall code rate ( $R^{\text{time}} \times R^{\text{space}} = R_s = 1/4$ ) as its time-domain 1-D counterpart as in Fig. 7. For instance, for a short length of  $N^{\text{time}} = 16$ , the performance gain of 2-D coding is more than 3 dB at FER =  $10^{-3}$ .

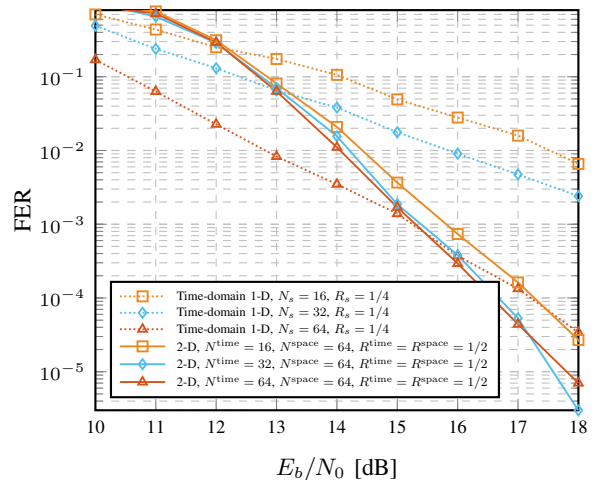


Fig. 9. FER performance comparison between the time-domain 1-D coding and spatiotemporal 2-D coding with different time-domain code lengths.



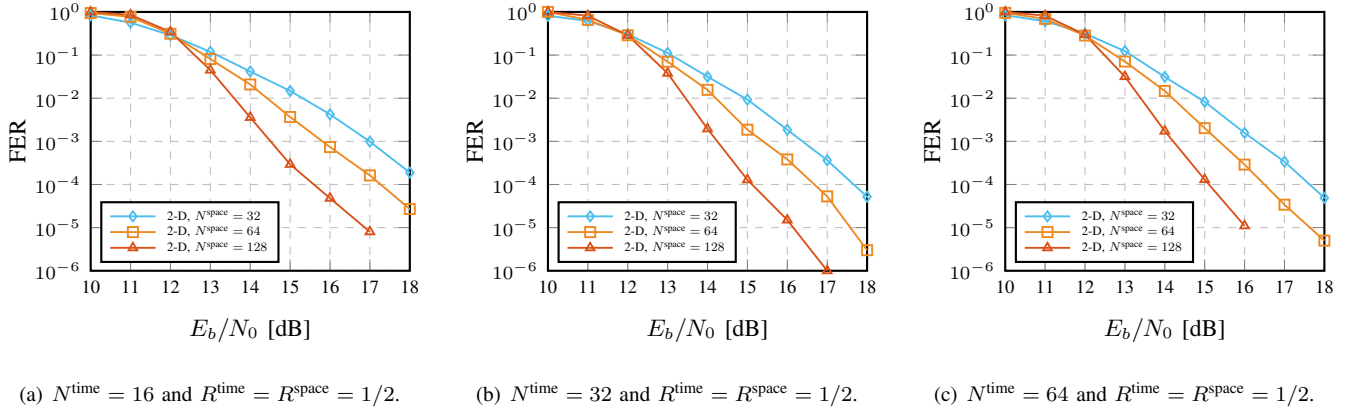


Fig. 10. FER performance comparison of the spatiotemporal 2-D coding with different space-domain code lengths.

### B. Space-Domain Coding Takes a Dominant Role

Fig. 9 offers us more information. Comparing error performance of spatiotemporal 2-D coding curves with different  $N^{\text{time}}$ , it is shown that the curve varies little while  $N^{\text{time}}$  changing. The reason is that the space-domain coding takes a dominant role in spatiotemporal coding when  $N^{\text{time}}$  is relatively small. As long as the space-domain coding stays the same, the performance stays similar, no matter how other parameters such as  $N^{\text{time}}$  change.

This observation inspires us to think of approaches to further improve the reliability of the spatiotemporal 2-D coding. Two immediate approaches are 1) increasing the space-domain code length  $N^{\text{space}}$ , and 2) reducing the space-domain code rate  $R^{\text{space}}$ .

### C. Increasing $N^{\text{space}}$ Improves the Reliability

According to the results in Fig. 10, it can be seen that for the same  $N^{\text{time}}$ , higher  $N^{\text{space}}$  brings higher reliability. This holds for different values of  $N^{\text{time}}$ . It is noted that here, in the three plots  $N_t = N_r/2 = N^{\text{space}}$ , and  $N_t \times N_r = 64 \times 128$  does not hold here. Therefore, for applications requiring higher reliability, designers can simply increase the number of antennas for space-domain coding.

### D. Decreasing $R^{\text{space}}$ Improves the Reliability

According to the results in Fig. 11, it can be seen that for the same  $N^{\text{time}}$  and  $N^{\text{space}}$ , lower  $R^{\text{space}}$  brings higher reliability. This holds for different values of  $N^{\text{time}}$ . It is noted that, for fair comparison, the time-domain code rate  $R^{\text{time}}$  increases while  $R^{\text{space}}$  decreasing, to make sure  $R^{\text{time}} \times R^{\text{space}} = 1/4$  is a constant. Therefore, for applications requiring higher reliability, designers can also decrease the code rate of space-domain coding.

### E. Commutativity of Time/Space-Domain Coding

According to Section III-C, it is known that the time-space mode and space-time mode are differentiated in the encoding order. Therefore, their performance will be similar, which is verified by Fig. 12. In real applications, users can decide to choose which one according to the specific requirements.

## V. DISCUSSIONS

In this section, some discussions are provided to offer useful insights for readers.

1) *Flexibility*: The application of the proposed coding scheme is not limited to the very low latency reliable MIMO transmission. This scheme can flexibly trade-off between latency and reliability by configuring the code rate, code length, and parameters  $S$  and  $T$ . For example, if  $S = 1$  and  $R^{\text{space}} = 1$ , the proposed spatiotemporal 2-D coding will become time domain 1-D coding, which is suitable for the eMBB case. In other words, the proposed scheme offers a uniform scheme which can meet the requirements of vast applications including both eMBB and URLLC cases.

2) *Versatility*: Though polar codes are employed as a running example for better understanding of the proposed scheme, the channel codes involved do not necessarily be polar codes and can be freely chosen. Second, the proposed scheme only focuses on the channel coding part of baseband processing, therefore can be directly used by any MIMO systems including 5G, 5G Evolution, 6G, and so on, without changing the other parts of the existing systems.

3) *Theoretical Basis*: The proposed coding scheme can be treated as the application of product codes and their variants in massive MIMO systems. Therefore, the proposed scheme can further vary based on similar codes such as interleaved codes, concatenated product codes, and so on. The existing results of coding theory can be used to further improve the proposed spatiotemporal 2-D coding.

4) *Implementations*: Thanks to the regular structure of the 2-D codeword trellis, the proposed coding scheme is implementation friendly. Still there are implementation issues required further research. One issue is the implementation of iterative decoder of the spatiotemporal 2-D codes. Another issue is how the choice of block partition of codeword trellis and specific codes will affect the implementation efficiency. For example, should the channel codes of both dimensions be the same or not? If not, how to improve the hardware utilization by module sharing?

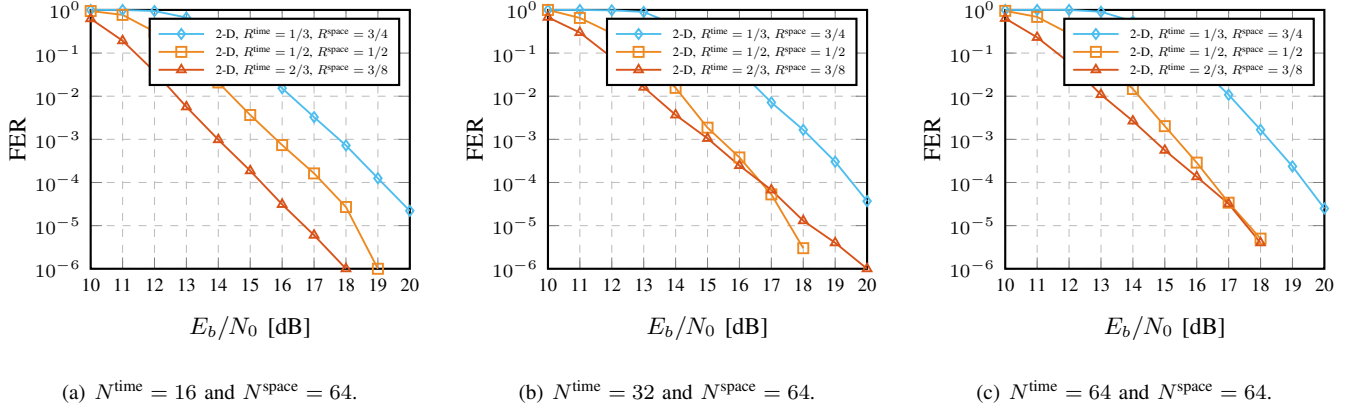


Fig. 11. FER performance comparison of the spatiotemporal 2-D coding with different space-domain code rates.

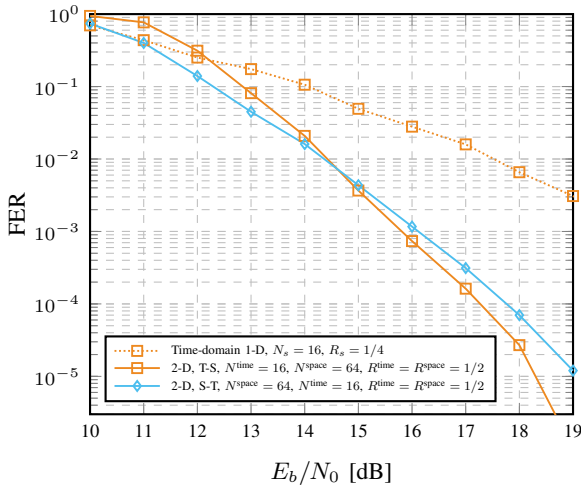


Fig. 12. FER performance comparison between the time-space (T-S) mode and the space-time (S-T) mode.

## VI. CONCLUSIONS

In this paper, a spatiotemporal 2-D channel coding is first proposed for very low latency reliable MIMO transmission. Numerical simulations have demonstrated its advantages of performance, latency, and flexibility over the state-of-the-art schemes. With good versatility, the proposed coding scheme has wide application prospect. Future work will be directed to the hardware implementations and systematic applications.

## VII. ACKNOWLEDGEMENT

The authors thank Huizheng Wang, Houren Ji, Xu Pang, and Leyu Zhang for their help in composing this paper.

## REFERENCES

- [1] 3GPP, "LTE Enhancements and 5G Normative Work. Release-15," 2018. [Online]. Available: <http://www.3gpp.org/release-15>
- [2] *Service requirements for 5G system: Stage 1*, 3GPP TS22.261 version 15.0.0, Mar. 2017.
- [3] *Study on scenarios and requirements for next generation access technologies*, 3GPP TR38.913 version 15.0.0, Jul. 2018.
- [4] *Study on new radio access technology physical layer aspects*, 3GPP: TR 38.802 version 14.2.0, Sep. 2017.
- [5] *5G NR: Multiplexing and channel coding*, 3GPP TS 38.212 version 15.2.0, Jul. 2018.
- [6] *Study on enhancement of Ultra-Reliable Low-Latency Communication (URLLC) support in the 5G core network*, 3GPP TR 23.725, Jun. 2019.
- [7] *Study on new radio (NR) access technology*, 3GPP TR 38.912 version 14.0.0, May. 2017.
- [8] X. You, "Shannon theory and future 6G," *SCIENTIA SINICA Informationis*, vol. 50, no. 9, p. 1377, 2020.
- [9] C. Zhang, Y.-H. Huang, F. Sheikh, and Z. Wang, "Advanced baseband processing algorithms, circuits, and implementations for 5G communication," *IEEE Trans. Emerg. Sel. Topics Circuits Syst.*, vol. 7, no. 4, pp. 477–490, 2017.
- [10] T. Jonna, S. K. Reddy, and J. K. Milleth, "Rank and MIMO mode adaptation in LTE," in *Proc. IEEE Inter. Conf. Adv. Net. Telecom. Syst. (ANTS)*, 2013, pp. 1–6.
- [11] *5G NR: Physical channels and modulation*, 3GPP TS 38.211 version 15.2.0, July 2018.
- [12] I. Tal and A. Vardy, "How to construct polar codes," *IEEE Trans. Inf. Theory*, vol. 59, no. 10, pp. 6562–6582, 2013.
- [13] E. Arıkan, "Channel polarization: A method for constructing capacity-achieving codes for symmetric binary-input memoryless channels," *IEEE Trans. Inf. Theory*, vol. 55, no. 7, pp. 3051–3073, 2009.
- [14] M. Tüchler, A. Singer, and R. Koetter, "Minimum mean squared error equalization using a priori information," *IEEE Trans. Signal Process.*, vol. 50, no. 3, pp. 673–683, 2002.
- [15] C. Studer, S. Fateh, and D. Seethaler, "ASIC implementation of soft-input soft-output MIMO detection using MMSE parallel interference cancellation," *IEEE J. Solid-State Circuits*, vol. 46, no. 7, pp. 1754–1765, 2011.
- [16] Q. Guo and D. D. Huang, "A concise representation for the soft-in soft-out LMMSE detector," *IEEE Commun. Lett.*, vol. 15, no. 5, pp. 566–568, 2011.